ELSEVIER

Journal of Alloys and Compounds 408–412 (2006) 33–36

Journal of ALLOYS AND COMPOUNDS

www.elsevier.com/locate/jallcom

X-ray resonant magnetic study of CePtSn

Blanka Janoušová[a,*], Carsten Detlefs[b], Stanislav Daniš[a], Jiří Prchal[a], Takemi Komatsubara[c], Vladimír Sechovský[a]

[a] *Department of Electronic Structures, Faculty of Mathematics and Physics, Charles University, 12116 Prague 2, Czech Republic*
[b] *European Synchrotron Radiation Facility, Boîte Postale 220, 38043 Grenoble Cedex, France*
[c] *Department of Physics, Graduate School of Science, Tohoku University, Sendai 980-8578, Japan*

Available online 14 June 2005

Abstract

The antiferromagnetic ground state of the equiatomic ternary intermetallic compound CePtSn was studied by means of X-ray resonant magnetic scattering. The Ce L_2 edge signal shows that below the Néel temperature (~ 7.5 K) an incommensurate magnetic structure with the propagation vector $\boldsymbol{q}_1$ varying monotonously between (0 0.415 0) at T_N and (0 0.417 0) at 5.0 K is present. At $T_M = 5$ K, the magnetic propagation vector locks in, and an additional Fourier component develops at $\boldsymbol{q}_2 = (0\ 0.47\ 0)$. Polarization analysis was used to determine the direction of the ordered Ce moments. Near the Pt L_3 edge, only non-resonant scattering could be observed, suggesting the induced moment at the Pt site to be negligible, as also indicated by band structure calculations.

PACS: 75.50.Ee; 75.60.Ch; 75.25.+z

Keywords: CePtSn; X-ray resonant magnetic scattering; Antiferromagnetic ordering; Magnetic structure; Cerium intermetallics

1. Introduction

CePtSn belongs to the family of ternary Ce compounds exhibiting intriguing electronic properties due to the competition of the RKKY interaction, the Kondo effect, and the crystal field (CF) interaction. The experimental value of the characteristic Kondo temperature for CePtSn, $T_K \sim 10$ K, is close to the Néel temperature $T_N = 7.5$ K [1]. CePtSn undergoes a second magnetic phase transition at $T_M = 5.0$ K.

CePtSn has been studied by a variety of techniques, including μSR [2], neutron scattering [3,4] and Mössbauer spectroscopy [5]. The magnetic structures and the nature of the magnetic phase transition at T_M remain undetermined. The aim of the present study is to answer these open questions.

The first neutron diffraction experiment [3] indicated an incommensurate magnetic structure with propagation $\boldsymbol{q}_1 = 0.418b^*$ at $T_M < T < T_N$ and $\boldsymbol{q}_2 = 0.466b^*$ below T_M and magnetic moment of $(0.84 \pm 0.08)\,\mu_B$ at $T = 2$ K and $(0.60 \pm 0.06)\,\mu_B$ at $T = 4.8$ K, respectively. These results are in contradiction to the zero-field μSR spectra [2] that display coherent oscillations indicating a locally commensurate ordering. A semi-quantitative model [6] describes the magnetic structure of CePtSn as a simple antiferromagnetic one with $\boldsymbol{q} = (0\,1/2\,0)$ with additional spin slips induced by the crystal field interaction [7]. Representation analysis of the symmetry-allowed magnetic structures suggests that the single-k commensurate structure belongs to the Γ_3 irreducible representation of the space group *Pnma* in the intermediate temperature region. With decreasing temperature, also the Γ_2 representation is present [6].

2. Experimental

Single-crystalline sample of CePtSn, used previously in a neutron diffraction experiment, has been grown in a tetra-arc furnace by a modified Czochralski method under Ar atmosphere from a stoichiometric melt of constituting materials.

* Corresponding author. Present address: European Commission, Joint Research Center, Institute for Transuranium Elements, 76344 Eggenstein-Leopoldshafen, Germany.
E-mail address: blanka@mag.mff.cuni.cz (B. Janoušová).

0925-8388/$ – see front matter © 2005 Elsevier B.V. All rights reserved.
doi:10.1016/j.jallcom.2005.04.106

The X-ray resonant magnetic scattering technique (XRMS) is a powerful method for the study of magnetic ordering in solids. The magnetic scattering cross-section can be enhanced by several orders of magnitude by tuning the incident photon energy to resonances at absorption edges [8–11], in particular the $M_{4,5}$ edges of actinides and the $L_{2,3}$ edges of lanthanides. Furthermore, the angular and polarization dependence of the resonant cross-section may be utilized to obtain information about the orientation of the magnetic moments [12–14].

The synchrotron experiments were carried out at the magnetic scattering beamline ID20 of the European Synchrotron Radiation Facility (ESRF). The samples were mounted on the cold finger of an Orange type liquid He bath cryostat. The base temperature of this configuration was approximately 1.7 K.

For most of the magnetic diffraction experiments presented in this report the photon energy was tuned to the maximum of the E1-resonance at the Ce L_2 edge (6.164 keV). The incident X-rays were polarized parallel to the horizontal scattering plane (π polarization), and a LiF(2, 2, 0) crystal was used to analyze the polarization of the scattered beam. Additional measurements were performed at the Pt $L_{2,3}$ edges.

3. Results

Upon cooling through the Néel transition, superstructure reflections of the form $\boldsymbol{G} \pm (0\ q\ 0)$ with $q_1 \cong 0.42$ develop ($\boldsymbol{G}$ is the reciprocal lattice vector). Below T_M a second family of reflections at $\boldsymbol{G} \pm (0\ q\ 0)$ with $q_2 \cong 0.47$ appears. These are consistent with long range antiferromagnetic order as previously observed by neutron scattering [3,4]. In the following, we present a detailed study of the magnetic peaks at $(0\,2 \pm q_{1,2}\,0)$ and $(0\,3 - q_{1,2}\,0)$.

3.1. Temperature dependence

The temperature dependence of the magnetic reflections $(0\,2 - q_{1,2}\,0)$ of CePtSn is summarized in Fig. 1. The data were taken at the Ce L_2 resonance. They confirm the results of our neutron diffraction studies but due to the much better Q-resolution of the XRMS method, give further information on the behaviour of the magnetic structure in this compound. The magnetic signal shows that below the Néel temperature (~ 7.5 K) an incommensurate magnetic structure with the propagation vector $\boldsymbol{q}_1$ varying monotonously between (0 0.415 0) at T_N and (0 0.417 0) at 5.0 K is present. At $T_M = 5$ K, the magnetic propagation vector locks in, the position and intensity of the q_1 satellites remain constant.

Furthermore, an additional Fourier component develops at $\boldsymbol{q}_2 = (0\ 0.47\ 0)$. The intensity of the q_2 peaks is approximately 1/20 of the q_1 peak. There is no observable change in the width of the reflections and it appears that both modulations coexist microscopically.

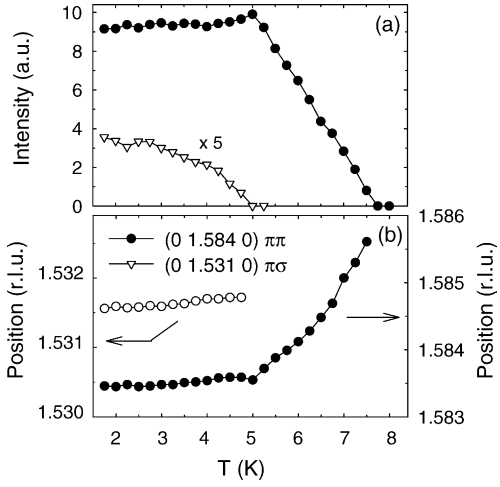

Fig. 1. The temperature dependence of the integral intensity of the two characteristic magnetic reflections in CePtSn (panel a) and of their reciprocal space position (panel b).

3.2. Polarization analysis

Polarization analysis was used to determine the direction of the ordered Ce moments. The magnetic resonant contribution to the coherent scattering amplitude in the electric dipole approximation $f_{n\mathrm{E1}}^{\mathrm{XRES}}$ can be written as [12]

$$\begin{pmatrix} f_\sigma \\ f_\pi \end{pmatrix} = iF^{(1)} \begin{pmatrix} 0 & \hat{\boldsymbol{k}} \cdot \hat{\boldsymbol{z}} \\ -\hat{\boldsymbol{k}}' \cdot \hat{\boldsymbol{z}} & (\hat{\boldsymbol{k}}' \times \hat{\boldsymbol{k}}) \cdot \hat{\boldsymbol{z}} \end{pmatrix} \begin{pmatrix} \epsilon_\sigma \\ \epsilon_\pi \end{pmatrix} \tag{1}$$

where $F^{(1)}$ is an amplitude factor, $\hat{\boldsymbol{k}}$ and $\hat{\boldsymbol{k}}'$ the incident and scattered beam directions, $\hat{\boldsymbol{z}}$ the unit vector in the direction of magnetic moment, and ϵ_π and ϵ_σ represent the incident polarization of the beam.

Since the incident polarization used in the present experiment was π, the magnetic resonant scattering amplitudes for σ and π polarized scattered beam are

$$\begin{aligned} f_\sigma &= \hat{\boldsymbol{k}} \cdot \hat{\boldsymbol{z}} \\ f_\pi &= (\hat{\boldsymbol{k}}' \times \hat{\boldsymbol{k}}) \cdot \hat{\boldsymbol{z}}. \end{aligned} \tag{2}$$

Therefore, the signal in the $\pi \rightarrow \sigma$ channel is proportional to the magnetic moments in the scattering plane, whereas the $\pi \rightarrow \pi$ channel contains information on the perpendicular component of the magnetic moment. More detailed data can be obtained by varying the relative orientation $\hat{\boldsymbol{z}}$ of the magnetic moments and the incident and scattered beam directions $\hat{\boldsymbol{k}}$ and $\hat{\boldsymbol{k}}'$. This "azimuthal scan" technique is often used for studies of orbital and/or quadrupolar order. In our experimental configuration changing the azimuth required warming up and remounting the sample, therefore only two settings were explored (see Fig. 2): the *b*–*c* and *a*–*b* scattering planes.

As can be seen from Fig. 3, in the intermediate temperature range $T_M < T < T_N$ the magnetic peak intensity for $\boldsymbol{Q} = (0\,2 + q_1\,0)$ is in the $\pi \rightarrow \pi$ channel, i.e. it

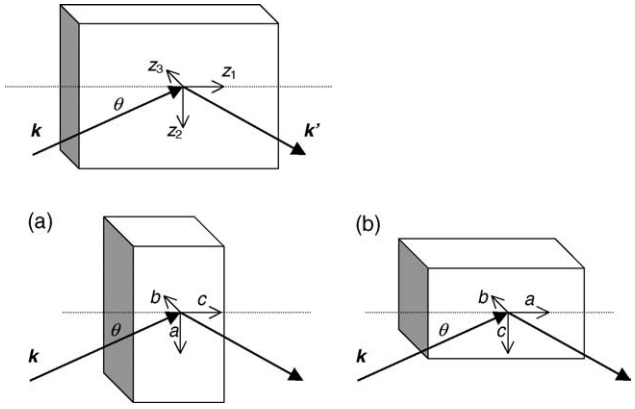

Fig. 2. Two scattering geometries used in the present experiment. Θ is the Bragg angle. $f_\sigma \propto \tilde{\mu} \parallel$ SP, i.e. b–c plane in geometry (a), and a–b in geometry (b). $f_\pi \propto \tilde{\mu} \perp$ SP, i.e. a-axis in geometry (a) and c-axis in geometry (b).

corresponds to a magnetic moment along the a-axis. The second Fourier component at $\boldsymbol{Q} = (0\ 3 - q_1\ 0)$ has opposite polarization, being entirely in the $\pi\rightarrow\sigma$ channel. This corresponds to magnetic moment confined in the b–c plane. Data from the second geometry (see Fig. 3c) shows the confinement in the a–b plane, thus indicating the b-axis direction. This magnetic peak originates from a lattice reflection forbidden by glide-plane extinction rule suggesting

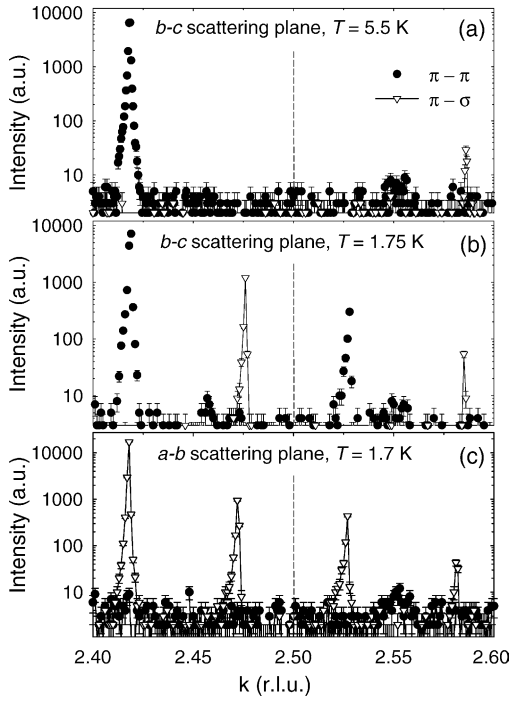

Fig. 3. K-scan of the representative magnetic reflections. The dashed line represents the Brillouin zone boundary at $k = 2.5$. In the first geometry ($a + b$), for $\boldsymbol{Q}_1 = 2.418b^*$ the signal is in the $\pi\rightarrow\pi$ channel which means moments perpendicular to the scattering plane ($\parallel a$-axis). For $\boldsymbol{Q}_2 = 2.585b^*$ the signal is only in the $\pi\rightarrow\sigma$ channel and the moments in the scattering plane (b–c plane). In the second geometry (c) all signal is in the $\pi\rightarrow\sigma$ channel, i.e. all magnetic moments are in the scattering plane (a–b plane).

antiferromagnetic ordering *within* the lattice unit cell along the b-axis.

The q_1-related reflections remain below T_M where also magnetic satellites corresponding to q_2 magnetic propagation appear. Also in this case the $(0\,2+q\,0)$ and $(0\,3-q\,0)$ magnetic reflections have opposite polarization. In the b–c scattering plane (SP) geometry they probe the Fourier components perpendicular to the scattering plane, i.e. along the crystallographic a-axis. In the a–b SP geometry (Fig. 3c), all peaks appear in the $\pi\rightarrow\sigma$ channel, indicating that all probed Fourier components $\tilde{\mu}$ lie within the SP. This is consistent with $\tilde{\mu}\parallel a$ for $(0\,2 + q_1\,0)$ and $(0\,3 - q_2\,0)$, and implies $\tilde{\mu}\parallel b$ for $(0\,3 - q_1\,0)$ and $(0\,2 + q_2\,0)$.

4. Discussion

The observation of the $(0\ 3 - q_{1,2}\ 0)$ magnetic reflections and the deduced orientations of the magnetic moment Fourier components allow us to make further conclusions on the magnetic structure of CePtSn. In the intermediate magnetic phase ($T_M < T < T_N$) we have one ferromagnetic Fourier component oriented along the crystallographic a-axis and one antiferromagnetic Fourier component oriented along the b-axis. The only combination of the symmetry-allowed basis vectors corresponds to the Γ_2 irreducible representation of the space group *Pnma*.

Similarly, the second magnetic propagation appearing below T_M has one ferromagnetic Fourier component parallel to the b-axis and an antiferromagnetic one along the a-axis. This case corresponds to the Γ_3 irreducible representation. Our results contradict the assignment of the Γ_3 irreducible representation to the intermediate and Γ_2 to the low-temperature phase given in Ref. [6].

From the intensity ratio of the two Fourier components in the intermediate temperature range we could deduce the angle between the local magnetic moment in the a–b plane and the crystallographic b-axis to be $(3.7 \pm 0.7)^\circ$.

Further inspection of the symmetry-allowed magnetic moment configuration for the two irreducible representations of the $(0\,k\,0)$-type reflections studied here (Γ_2 and Γ_3) reveals that the structure factor vanishes for the c-axis component of the magnetic moment so that our measurements are not sensitive to an eventual c-axis contribution. Macroscopic magnetization measurements however show the c-direction as the hard axis therefore no c-axis component of the magnetic moment is expected.

A more detailed data analysis based on the irreducible representation analysis will be published in the near future.

In the present experiment, we have also studied the Pt L_3 edge. Near the absorption edge, only non-resonant scattering could be observed suggesting that the induced moment at the Pt site is negligible, as also indicated by XMCD results and band structure calculations [15].

Acknowledgements

This work is a part of the research program MSM 0021620834 that is financed by the Ministry of Education of Czech Republic. Partial support comes also from the Grant Agency of the Czech Republic (Grant no. 202/02/0739) and the Grant Agency of the Charles University (Grant no. 282/2004/B-FYZ/MFF).

We acknowledge the ESRF for provision of beamtime on ID20.

References

[1] T. Takabatake, H. Iwasaki, G. Nakamoto, H. Fujii, H. Nakotte, F.R. de Boer, V. Sechovský, Physica B 183 (1993) 108.
[2] G.M. Kalvius, A. Kratzer, K.H. Münch, F.E. Wagner, S. Zwirner, H. Kobayashi, T. Takabatake, G. Nakamoto, H. Fujii, S.R. Kreitzman, R. Kiefl, Physica B 186–188 (1993) 412.
[3] H. Kadowaki, T. Ekino, H. Iwasaki, T. Takabatake, H. Fujii, J. Sakurai, J. Phys. Soc. Jpn. 62 (1993) 4426.
[4] B. Janoušová, P. Svoboda, V. Sechovský, K. Prokeš, T. Komatsubara, H. Nakotte, S. Chang, B. Ouladdiaf, I. Císařová, Appl. Phys. A 74 (2002) S731.
[5] H. Kobayashi, F.E. Wagner, G.M. Kalvius, T. Takabatake, Hyperfine Interact. 93 (1994) 1515.
[6] H. Kadowaki, J. Phys. Soc. Jpn. 67 (1998) 3261.
[7] D.R. Noakes, G.M. Kalvius, Physica B 289 (2000) 248.
[8] M. Blume, J. Appl. Phys. 57 (1985) 3615.
[9] D. Gibbs, D.R. Harshman, E.D. Isaacs, D.B. McWhan, D. Mills, C. Vettier, Phys. Rev. Lett. 61 (1988) 1241.
[10] J.P. Hannon, G.T. Trammell, M. Blume, D. Gibbs, Phys. Rev. Lett. 61 (1988) 1245.
[11] E.D. Isaacs, D.B. McWhan, D.P. Siddons, J.B. Hastings, D. Gibbs, Phys. Rev. Lett. 40 (1989) 9336.
[12] J.P. Hill, D.F. McMorrow, Acta Cryst. A 52 (1996) 236.
[13] C. Detlefs, A.I. Goldman, C. Stassis, P.C. Canfield, B.K. Cho, J.P. Hill, D. Gibbs, Phys. Rev. B 53 (1996) 6355.
[14] C. Detlefs, A.H.M.Z. Islam, A.I. Goldman, C. Stassis, P.C. Canfield, Phys. Rev. B 55 (1997) R680.
[15] B. Janoušová, F. Wilhelm, N. Jaouen, A. Rogalev, V. Sechovský, Physica B 359–361 (2005) 127.